

Detailed Analysis of Backward Facing Step with Different Turbulence Models and Laminar Flow – Reattachment and Recirculation Point

Author: Danya lincy T J
School of Engineering and Computer Science
University of Hertfordshire

Abstract:- The CFD analysis of flow over a two dimensional backward facing step model having an expansion ratio is done by using Star CCM+. The velocity distribution, recirculation, and reattachment over different models of turbulent and laminar is analysed. In this analysis the velocity is calculated with Reynolds number of Turbulence and laminar. In Turbulence K-epsilon, K-omega, S-A Turbulence models' computations are performed, and the results are compared in accordance with Navier-stokes equation. The laminar model is also analysed, and comparison of laminar and turbulence flow is Concluded. The Reattachment length is calculated and compared for all the turbulence and laminar models.

Keywords:- Star CCM+, Reynolds number, Expansion ratio, Recirculation and Reattachment

I. INTRODUCTION

Computational Fluid Dynamics (CFD) is a branch of Fluid Dynamics which is used for numerical analysis and algorithms to solve and analyse problems in which fluid flows are involved. Commercial software packages like ANSYS Fluent and STAR CCM+ are used for performing simulation and numerical analysis in defined boundary conditions for the flow of gases and liquids. This analysis is usually used in Aerospace and Automotive industries. In fluid mechanics Flow through a backward facing step is one of the classical internal flow problems. Due to simplistic geometry and flow characteristics, this circumstance has become a practice for numerical validation in CFD.

Recirculating and Reattachment flow over backward facing step (BFS) has been a benchmarking geometry for numerical and experimental turbulence flow study. Backward facing-step (BFS) is probably the most used and standard geometry for numerical CFD and experimental flow analysis which includes laminar flow, recirculating turbulent model verification in 2-D and 3-D geometry. There are many complicated turbulent flows occurring in many engineering and industrial conditions that involves heat transfer; sudden expansion cause recirculating flow, flow separation, large pressure gradient these all can be represented in BFS geometry, both. numerically and experimentally. Researchers have used BFS to analyse the complex flow in electronic cooling and advanced

applications such as combustion chamber, turbines in gas turbine, nuclear reactors and magneto hydrodynamics flow and Nano-fluid flows (Ramsak, 2015; Gautier & Aider, 2014) and many engineering applications, ranging from various fluidic elements, cooling of turbine blades, air conditioning pipelines, to numerous devices. BFS can be found in many technical applications in mechanical and civil engineering.

BFS is an interesting case for studying the performance and solution strategy of a turbulent model. In this case, the flow is subjected to a sudden increase of cross-sectional area result in a separation of the flow starting at point of expansion. Spatial variation in velocity field cause production of turbulence outside the wall region and its interaction with mean flow influences the size of re-attachment length. The size of re-attachment length is one of the most important quantities that must be predicted accurately by turbulence model.

As there are many variations of the BFS geometry's parameters, only few parameters we considered such as inlet velocity, outlet pressure, step height, expansion ratio. Both experimental and numerical methods are reviewed. The experimental conditions of BFS are for 2-D.

II. LITERATURE VIEW

Mohammad A. Hossain, M. T. (2013). Backward Facing Step Channel. Numerical Investigation of Fluid Flow through a 2D Backward Facing Step Channel.

In this paper a 2D planner pressure-based solver is used for the simulation. Water is considered as a working fluid. Inlet boundary condition is based on Re. In this case the pressure outlet is assumed constant. To validate the CFD model, flow separation length (X_r/h) at different Re is compared with experimental data. Horizontal and vertical velocity is calculated for different Re ranging from 100 to 4000 to observe the flow behaviour in laminar, Transition and the turbulent regimes. For Laminar flow there is a single flow separation at the step when Re (100 – 300), the length of separation increases as Re increases. The second separation occurs at Re = 350. The separation length varies with Re, and flow becomes more unstable. Then Re increases from transition to turbulent. The flow separation at Re = 4000 is considered as Turbulent flow. In this literature CFD simulation is done for the backward facing step for the

different Re to understand the flow behaviour for laminar, transition and turbulent flow. The result mesh independency test is tested. The separation length is calculated and compared with experimental data to verify the simulation result. Finally horizontal, vertical velocity contour and velocity distribution along with channel is calculated.

Senan Thabet, T. H. (2018). Analysis of a Backward Facing Step Flows. CFD Analysis of a Backward Facing Step Flow.

In this paper the CFD package is known as the solver code, reads the grids and setup information, solves the equation, and produces a result file containing the predicted flow characteristics. It may also take a larger number of computer servers to work for hours because the grid can be very large. Backward stepping measurement of the WIND code versus Perfect Gas Supersonic flow is validated. The Wind code with regional boundary conditions is used to determine the geometrical supersonic flow to compare with the data provided. The test case chosen is to enter traffic Mach number of 2.5 (Re = 460,000/in). Under these tunnel condition most of the upstream plate should be laminar. The transition to turbulent condition should occur on the background shear layer. In comparison of earlier version of NPARC and WIND with experimental data, the Wind code slightly overestimates the surface pressure drop from the free flow value to about 5% of the corner value of the separation area (bases pressure). This may be since the transition point is experimentally unknown and not accurately predicted by the natural transition of the Turbulence model. However, this over forecasting predicts the pervious pressure drop closer to the experiments results than AEDC, PARC, TUFF, and GASP code using the Baldwin Lomax. The rest of the forecast for WIND pressure is good agreement with the forecast pressure.

III. GEOMETRY

The flow domain geometry is modelled computationally using STRA CCM++.The Geometry of the backward facing step is developed using a step height of the model. Here we have taken the step height as 0.2 m. To get the accurate CFD flow behaviour the upward and downstream length is extended from the given length. To measure the accuracy of the flow the plane section is created at -0.5, -1, -1.5. The Geometry is given in the figure: 1. the Expansion ratio is taken as 2:3.

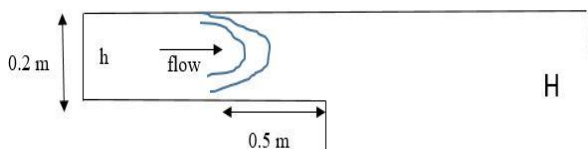


Figure 1: Geometry of backward facing step.

Upstream Height (m)	Downstream Height(m)	Step height(m)
6	3	0.2

Table: 1 Dimensions of BFS

IV. MESHING

Since it is a 2D modelling 2D badging of meshing is done first and for the volume mesh the Surface remeshers and trimmed cell meshers are used to create the meshing of the geometry. The base size of the mesh is taken as 0.001 m to get the fine mesh surface which provides more accurate results.

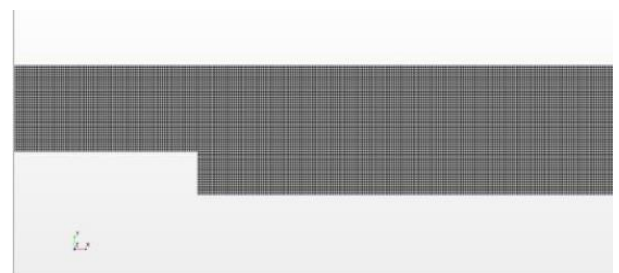


Figure 2: Meshing of BFS

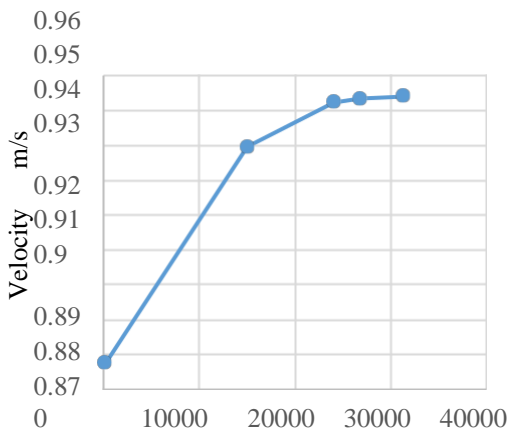
V. MESH INDEPENDENCY CHECK

To make the solution more independent to the mesh we must carry out the mesh independency check. we must make sure the convergence of the residual error to 10-4 (Team, 2012). When the convergence criteria are obtained the mesh should be refined globally to get the finer cells of mesh. The mesh should be refined until the error is reduced. The mesh independency was met at around 31317 cells (Figure: 3)

No of cells	velocity	error
210	0.877503	
15000	0.93961	7%
24000	0.952343	1%
26800	0.95345	0%
31317	0.954061	0%

Table: 2 Mesh Independency: No of cells vs Velocity

Mesh Independency No of cells vs Velocity m/s



No of cells

Figure 3: No of cells vs Velocity m/s

VI. BOUNDARY CONDITIONS

At boundaries of the flow domain and zones we need to apply the numerical conditions the inlet is taken as velocity inlet and the value of velocity needs to be calculated from the desired Reynolds number for laminar and turbulent flow. The outlet is taken as pressure outlet with the constant value. The Reynolds number taken for laminar is 650 and the Reynolds number taken for turbulence is 21000.

Velocity for laminar:

$$v = \frac{Re \times \mu}{\rho \times D_H}$$

Re= Reynolds Number μ =Dynamic Viscosity Pa-s
 ρ =Density kg/m³ Dh=Hydraulic Diameter

The hydraulic diameter is calculated from the step height.

$$Dh = 2 \times h \text{ (B. F. ARMALYT, 1983)}$$

$$= 2 \times 0.2 = 0.4 \text{ m}$$

The dynamic viscosity and density values are constant.

$$\mu = 1.85508E-5 \text{ Pa-s}$$

$$\rho = 1.18415 \text{ kg/m}^3$$

From that the velocity for laminar is calculated as 0.025457 m/s

Velocity for Turbulence flow,

With the same method as laminar the velocity for Turbulence flow is calculated with the turbulence Reynolds number as 0.822461 m/s.

VII. TURBULENCE MODELS

Turbulence is a common phenomenon in fluid flow. Hinze (1975) presents a formal Turbulence is defined as: "a variety of irregular flow conditions the number shows random changes with time and space coordinates, and thus statistically different averages can be seen (Senan Thabet1, 2018). There are basic models in Turbulence are Reynolds-average Navier-Stokes's equations (RANS), direct numerical simulation (DNS), a large eddy simulation (LES). In Turbulence we are going to analysis three models which comes under the Reynolds-average Navier-Stokes's equations.

By decomposing each solution variable (Φ) Navier stokes equation into mean, averaged value ($\bar{\Phi}$) and the component of fluctuation (Φ') the Reynolds-average Navier-Stokes's equations are obtained.

$$\Phi = \bar{\Phi} + \Phi' \tag{1}$$

By inserting the decomposed solution variable in Navier stokes equation, the mean quantities equation is obtained.

The equation for mean mass and momentum is given by,

$$\frac{\partial \rho}{\partial t} + \nabla \cdot (\rho \bar{\mathbf{v}}) = 0$$

$$\frac{\partial}{\partial t} (\rho \bar{\mathbf{v}}) + \nabla \cdot (\rho \bar{\mathbf{v}} \otimes \bar{\mathbf{v}}) = - \nabla \cdot \bar{\mathbf{p}} \mathbf{I} + \nabla \cdot (\mathbf{T} + \mathbf{T}_{RANS}) + \mathbf{f}_b$$

----- (2) (Alfonsi, 2009)

Where?

ρ = density

$\bar{\mathbf{v}}$ mean velocity

$\bar{\mathbf{p}}$

= mean pressure \mathbf{I} = Identity tensor \mathbf{T} = Viscous tensor

\mathbf{f}_b = resultant of gravity and centrifugal forces

Based on the Reynolds-average Navier-Stokes three models (are analysed in STAR CCM+. The three models are.

- K-Omega model
- K-epsilon model
- Spalart –Allmaras Model

K-epsilon model and its Results:

The Reynolds number for turbulence is taken as 21000. With the Reynolds number the velocity was calculated. The k-ε model comes under the two-equation model and it is the most widely used model. The k is denoted by Turbulence kinetic energy and the ε is denoted by kinetic dissipation rate.

K- equation:

$$\frac{\partial k}{\partial t} + \bar{u}_j \frac{\partial k}{\partial x_j} = \frac{\partial}{\partial x_j} \left[\frac{(v + v_t)}{\sigma_k} \frac{\partial k}{\partial x_j} \right] - \epsilon + \tau_{ij} \frac{\partial \bar{u}_i}{\partial x_j}$$

----- (3) (Markatos, 2014)

ε- Equation

$$\frac{\partial \epsilon}{\partial t} + \bar{u}_j \frac{\partial \epsilon}{\partial x_j} = \frac{\partial}{\partial x_j} \left[\frac{(v + v_t)}{\sigma_\epsilon} \frac{\partial \epsilon}{\partial x_j} \right] + C_{\epsilon 1} \frac{\epsilon}{k} \tau_{ij} \frac{\partial \bar{u}_i}{\partial x_j} - C_{\epsilon 2} \frac{\epsilon^2}{k}$$

----- (4) (Markatos, 2014)

This model is mostly used to predict the shear flows and for the flow field estimation.

With the initial velocity of 0.82246 m/s the simulation results are obtained from start CCM+. The maximum velocity for this model obtained from the result is 0.94261 m/s. The model is iterated to 15000 steps and the residual is shown in figure: 4. The flow developed is shown in figure: 5 & 6.

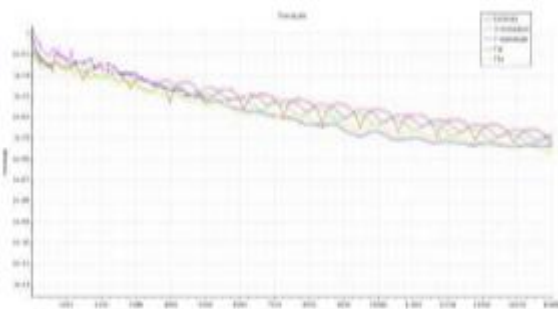


Figure 4: Residuals of K-epsilon Model

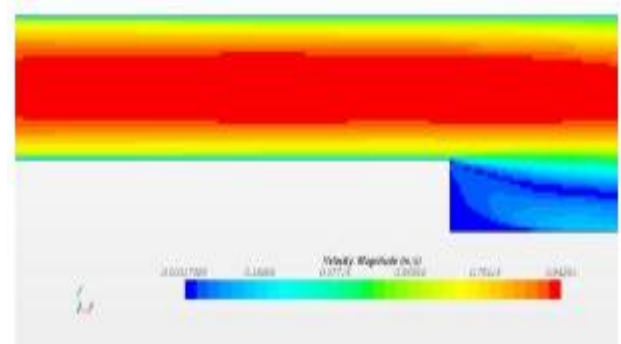


Figure 5: Scalar scene 1 of K-epsilon Model

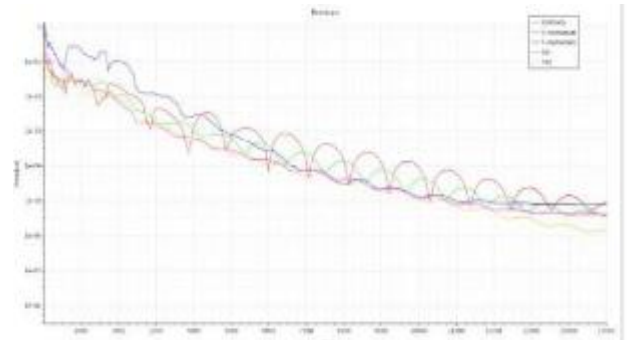


Figure 6: Scalar Scene 2 of K-epsilon model

K-Omega Model and its Results:

The K-Omega model comes under the two-equation model. The K is denoted as turbulent kinetic energy and the ω is denoted by specific dissipation rate.

K- equation:

$$\frac{\partial k}{\partial t} + \bar{u}_j \frac{\partial k}{\partial x_j} = \frac{\partial}{\partial x_j} \left[\left(v + \sigma^* \frac{k}{\omega} \right) \frac{\partial k}{\partial x_j} \right] - \beta^* k \omega + \tau_{ij} \frac{\partial \bar{u}_i}{\partial x_j}$$

----- (5) (Markatos, 2014)

ω- Equation:

$$\frac{\partial \omega}{\partial t} + \bar{u}_j \frac{\partial \omega}{\partial x_j} = \frac{\partial}{\partial x_j} \left[\left(v + \sigma \frac{k}{\omega} \right) \frac{\partial \omega}{\partial x_j} \right] - \beta \omega^2 + \frac{\sigma_d}{\omega} \frac{\partial k}{\partial x_j} \frac{\partial \omega}{\partial x_j} + a \frac{\omega}{k} \tau_{ij} \frac{\partial \bar{u}_i}{\partial x_j}$$

----- (6) (Markatos, 2014)

The k- ω model is more accurate for free shear flows.

With the initial velocity of 0.82246 m/s the simulation results are obtained from start CCM+. The maximum velocity for this model obtained from the result is 0.96136 m/s. The model is iterated to 15000 steps and the residual is shown in figure: 7. The flow developed is shown in figure: 8 & 9.

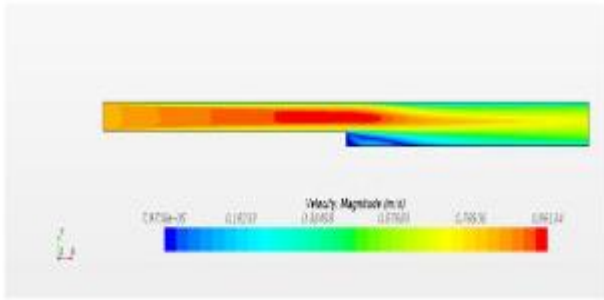


Figure 7: Residuals of k-omega Model

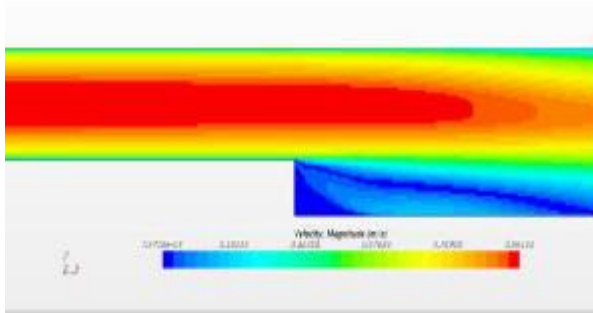


Figure 8: scalar scene 1: k-omega Model

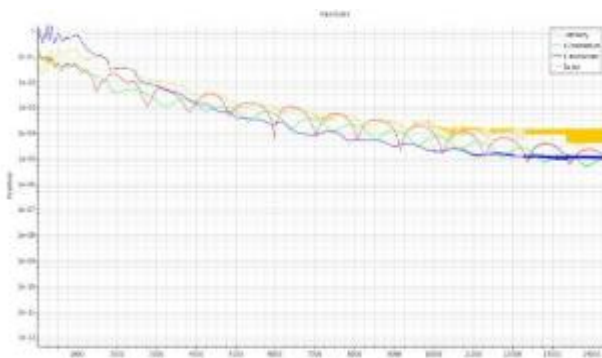


Figure 9: Scalar scene 2 k-omega Model

Spalart –Allmaras Model and its Results:

It is a one equation model and kinematic turbulence viscosity is solved from this equation. This model is less sensitive to numerical errors. The Spalart –Allmaras Model is given by.

$$\frac{\partial}{\partial t}(\rho \tilde{\nu}) + \frac{\partial}{\partial x_i}(\rho \tilde{\nu} u_i) = G_{\nu} + \frac{1}{\sigma_{\tilde{\nu}}} \left[\frac{\partial}{\partial x_j} \left\{ (\mu + \rho \tilde{\nu}) \frac{\partial \tilde{\nu}}{\partial x_j} \right\} + C_{b2} \rho \left(\frac{\partial \tilde{\nu}}{\partial x_j} \right)^2 \right] - Y_{\nu} + S_{\tilde{\nu}}$$

----- (7) (Anon., 2009)

With the initial velocity of 0.82246 m/s the simulation results are obtained from start CCM+. The maximum velocity for this model obtained from the result is 0.92685m/s. The model is iterated to 15000 steps and the residual is shown in figure:

10.The flow developed is shown in figure: 11&12 0.0377758 m/s. The model is iterated to15000 steps and the residual are shown in Figure: 13. The flow developed is shown in figure: 14&15

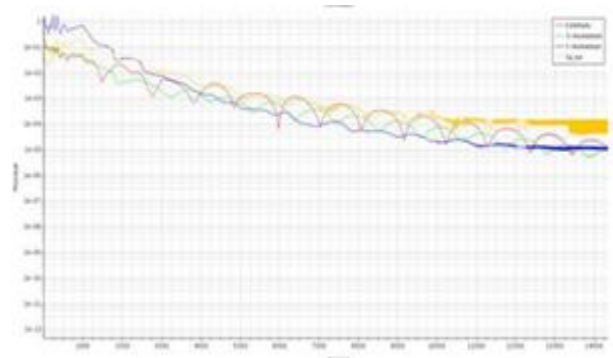


Figure 10: Residuals for Spalart-Allmaras Model

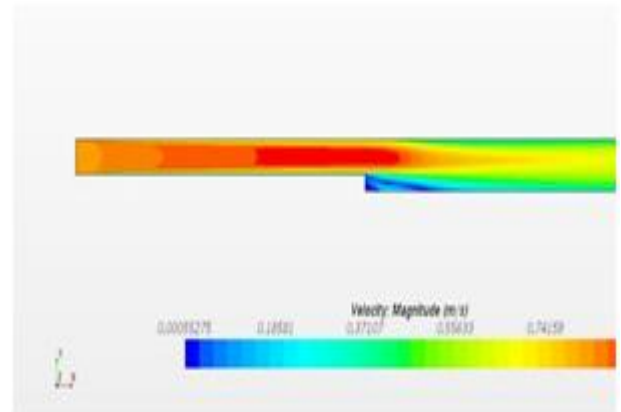


Figure 11: Scalar scene 1 Spalart-Allmaras Model

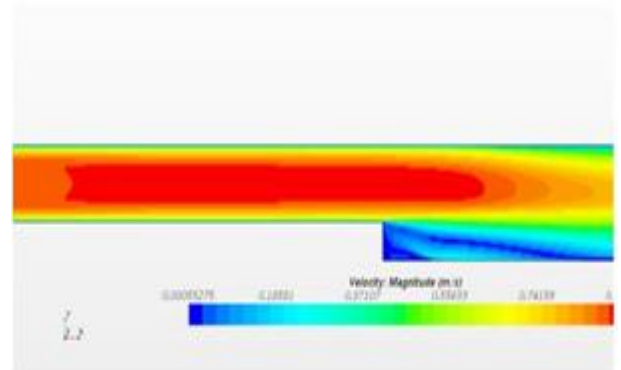


Figure 12: Scalar scene 2 Spalart-Allmaras Model

VIII. LAMINAR MODEL AND ITS RESULTS

In Laminar flow when a fluid flows, each particle of the fluid follows a smooth path which never interfere with one another. The velocity of the fluid is constant at any point in the fluid. At low velocity, the fluid tends to flow without the lateral mixing. The motion of the particles of the fluid will move in a straight line parallel to the pipe wall. This can be easily observed in enclosed pipes.

With the initial velocity of 0.02546 m/s the simulation results are obtained from start CCM+. The maximum velocity for this model obtained from the result is.

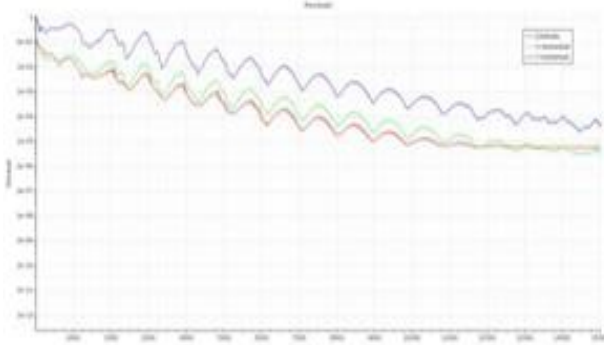


Figure 13: Residual of laminar Model

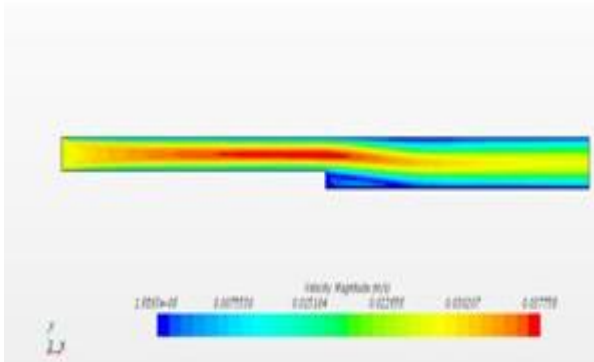


Figure 14: Scalar scene 1 laminar Model

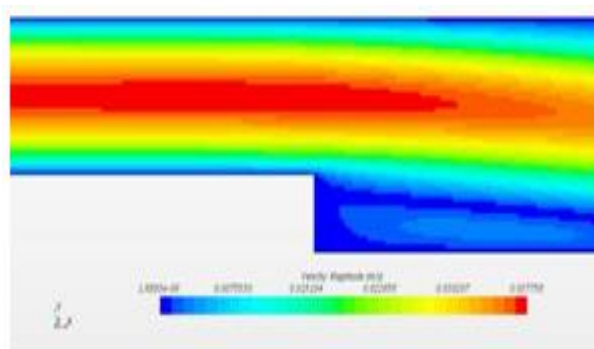


Figure 15: Scalar scene 2 Laminar Model

IX. RECIRCULATION AND REATTACHMENT

The recirculation of the flow is mainly formed as rotational vortexes (Figure: 16). The recirculation flow is depending on the step height (h). When recirculation zone ends the wake, reattachment occurs when the expansion ratio increases the reattachment length increases. The recirculation and reattachment are mainly considered as the representative parameters of the backward facing step. The reattachment and the recirculation zone depends on the step height, upstream height, and the expansion ratio.

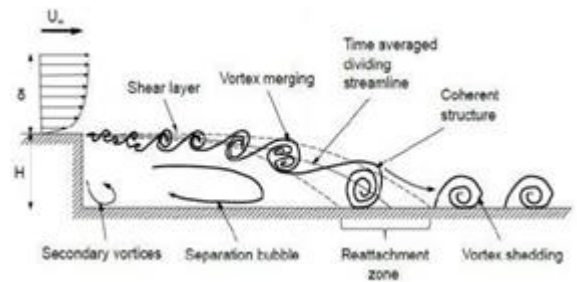


Figure 16: Reattachment and Recirculation Flow over Backward facing step (Darmawan, 2016)

The Reattachment and Recirculation developed in the Turbulence models are given in figure (17-19) and laminar models are given in figure: 20.

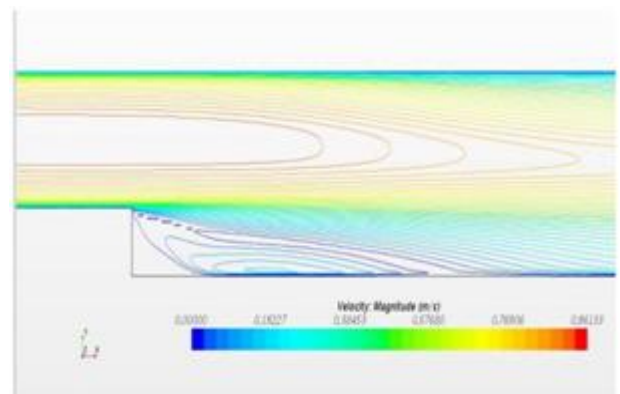


Figure 17: Reattachment and Recirculation of K-Omega Model

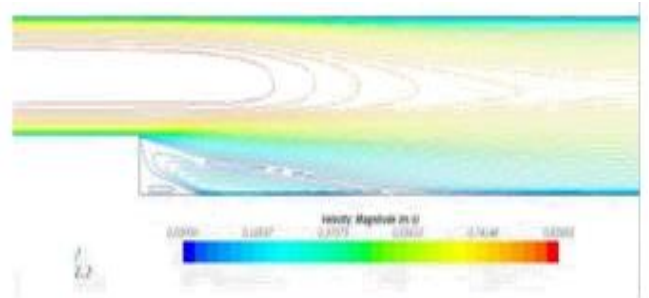


Figure 18: Reattachment and Recirculation of Spalart-Allmaras Model

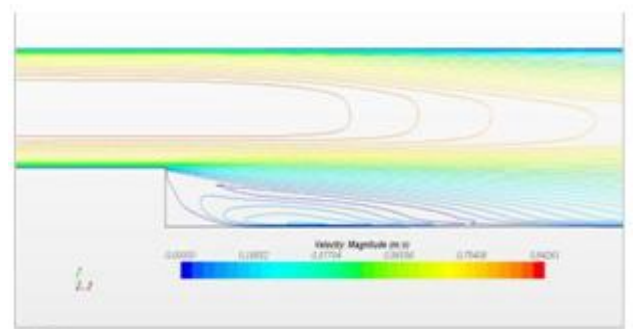


Figure 19: Reattachment and Recirculation of k-epsilon Model

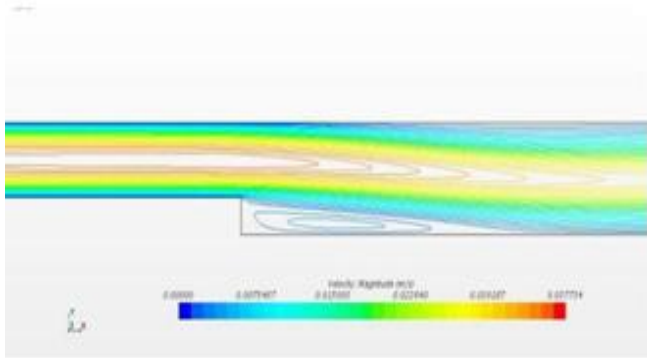


Figure 20: Reattachment and Recirculation of Laminar Model

The reattachment length is calculated from the wall shear stress and the direction graph shown in the figure (21-24). The negative coordinate depicts the recirculation and the positive coordinate depicts the reattachment zone.

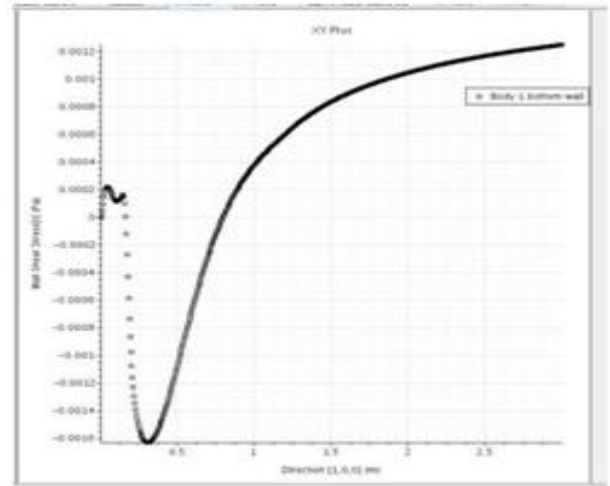


Figure 23: Wall shear stress vs Direction for Spalart-Allmaras Model

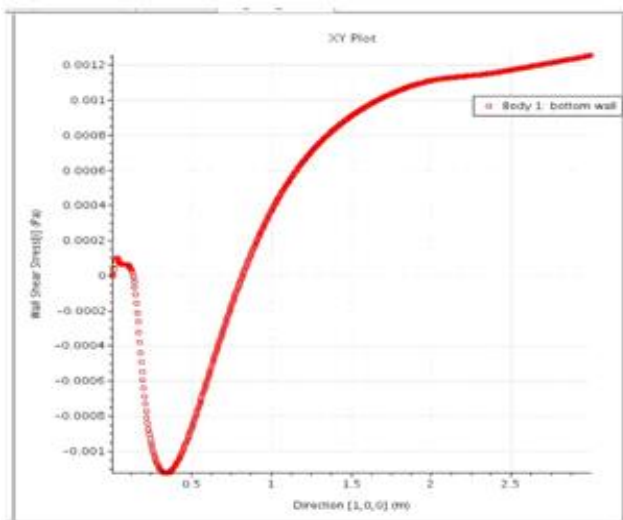


Figure 21: Wall shear stress vs Direction for k-epsilon Model

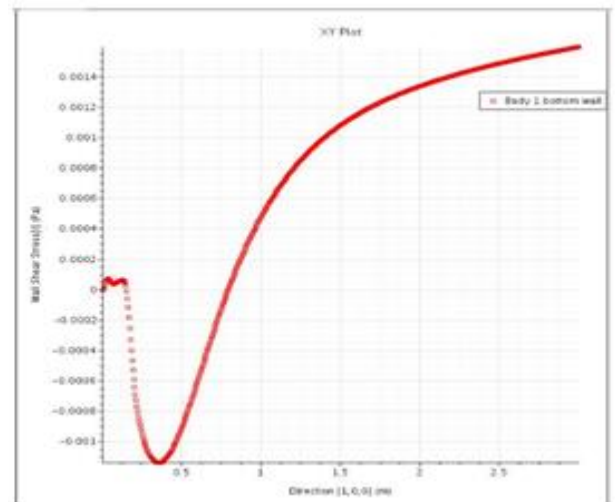


Figure 24: Wall shear stress vs Direction for K-omega Model

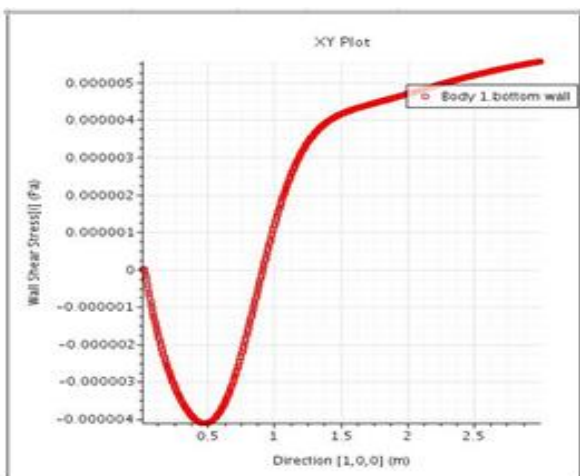


Figure 22: Wall shear stress vs Direction for laminar Model

X. COMPARISON OF TURBULENCE AND

Laminar flow

One of the major differences between laminar and turbulence is velocity profile. The velocity profile for laminar is parabolic and low velocity whereas in Turbulence the velocity profile is flat and has high velocity. We have created three planes at -0.5(plane section), -1(Plane section 2), -1.5(Plane section 3) for the accuracy of the result. The exact flow will be developed at -0.5. The graphs are included for three plane sections Refer Figure 25 to 27 for Turbulence model and Refer Figure 28 for Laminar Model. The Reattachment length for laminar Refer Figure: 29 is greater than the reattachment length of Turbulence models.

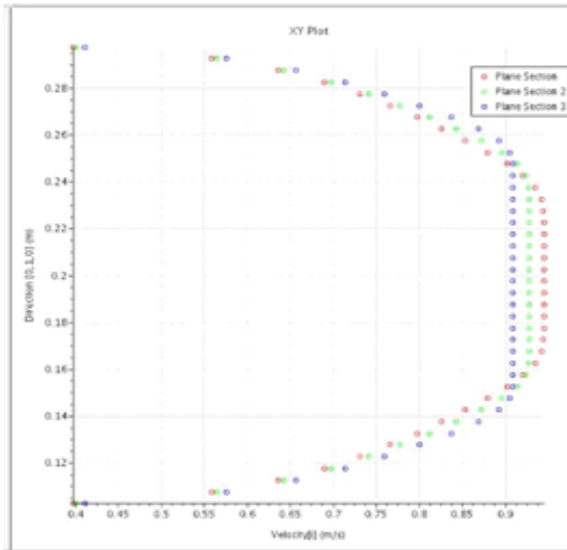


Figure 25: Velocity Profile for K-Omega Model

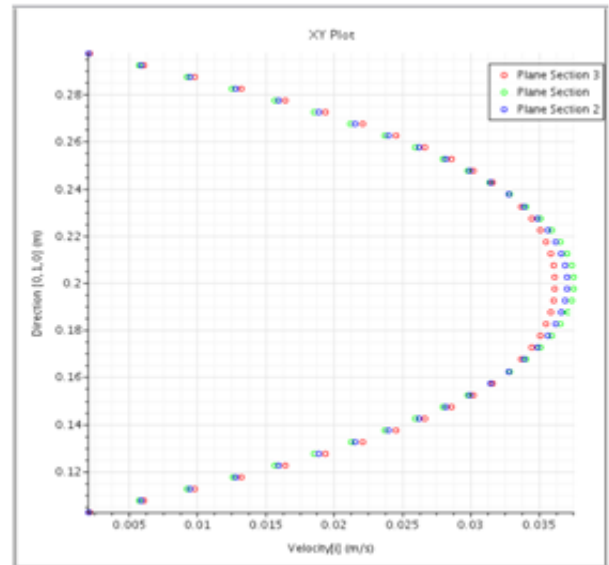


Figure 28: Laminar Model

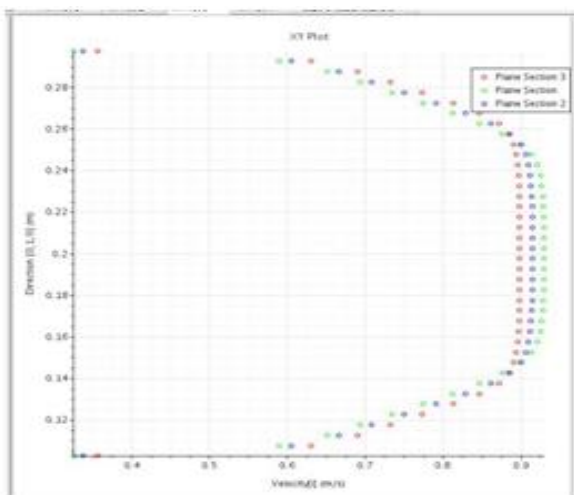


Figure 26: Velocity Profile for K-epsilon Model

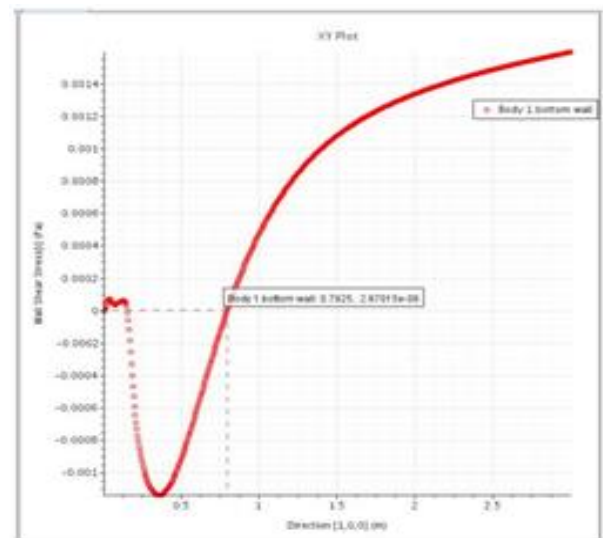


Figure 29: Reattachment length of laminar Model

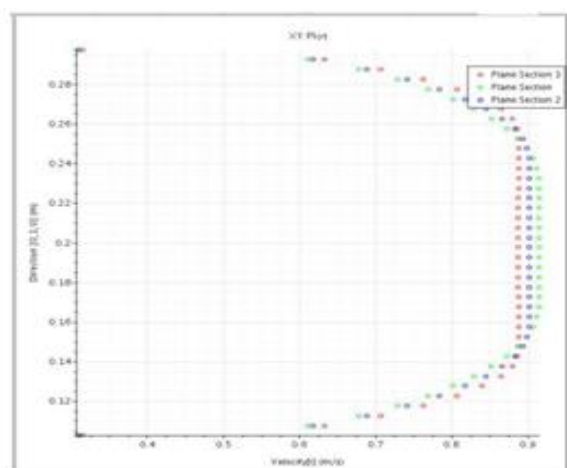


Figure 27: Velocity Profile for Spalart-Allmaras Model

XI. COMPARISON OF THREE MODELS OF TURBULENCE FLOW

K-ε and K-ω model obtain sort of similar results when compared to Spalart – Allmaras Model. Since K-ε and K-ω are two equation model and Spalart –Allmaras Model is one equation model. K-ω has highest velocity of 0.96134m/s than K-ε. and Spalart–Allmaras model. The reattachment length is maximum in K-ε. See Table: 3 and Refer figure 30-32. The K-and K-ω model has good computational results and accuracy than Spalart –Allmaras Model. Therefore, in most of the industries the K-ε and K-ω model are used.

Model	Reattachment Length
Turbulence (k- ω)	0.7925 m
Turbulence(k- ϵ)	0.8175 m
Turbulence(S-A)	0.7975 m
Laminar	0.9025 m

Table 3: Comparison of Reattachment length

XII. CONCLUSION

CFD simulation has been done for backward facing step for different models of turbulence and laminar to understand the flow behaviour. Mesh Independency test has been performed for different base size of mesh to get more accurate results. Velocity profiles of turbulence and laminar model was obtained and analysed. The recirculation and reattachment zones have been examined for both Turbulence and Laminar Models. From the above analysis we concluded that K- ϵ and K- ω models are better than Spalart

–Allmaras model.

REFERENCES

- [1]. Alfonsi, G., 2009. Reynolds-Averaged Navier-Stokes Equations for Turbulence Modeling. *Applied Mechanics Reviews*, p. 21.
- [2]. Anon., 2009. *ENEA GRID*. [Online] Available at: <https://www.afs.enea.it/project/neptunius/docs/fluent/html/th/node48.htm>
- [3]. B. F. ARMALYT, F. D. J. C. F. P. A. B. S., 1983. Experimental and theoretical investigation of backward-facing step flow. *J. Fluid Mech*, p. 24.
- [4]. Darmawan, S., 2016. BACKWARD FACING STEP GEOMETRY FOR FLOW ANALYSIS: AREVIEW OF. March, p. 13.
- [5]. Markatos, C. A., 2014. Recent advances on the numerical modelling of turbulent flows.elsevier, p. 40.
- [6]. Mohammad A. Hossian, M. T. R. S. R., 2013. Backward Facing Step Channel. Numerical Investigation of Fluid Flow through a 2D
- [7]. Backward Facing Step Channel.
- [8]. Senan Thabet1, T. H. T. a. Y. A. J., 2018. CFD
- [9]. Analysis of a Backward Facing Step Flows.
- [10]. INTERNATIONAL JOURNAL OF AUTOMOTIVE SCIENCE AND TECHNOLOGY, p. 7.
- [11]. Senan Thabet, T. H. T. a. Y. A. J., 2018. Analysis of a Backward Facing Step Flows. CFD Analysis of a Backward Facing Step Flow.
- [12]. Team, L. C., 2012. LEAP’s Computational Fluid Dynamics (CFD) Blog. [Online]
- [13]. Available at: <https://www.computationalfluidynamics.com.au/convergence-and-mesh-independent-study>

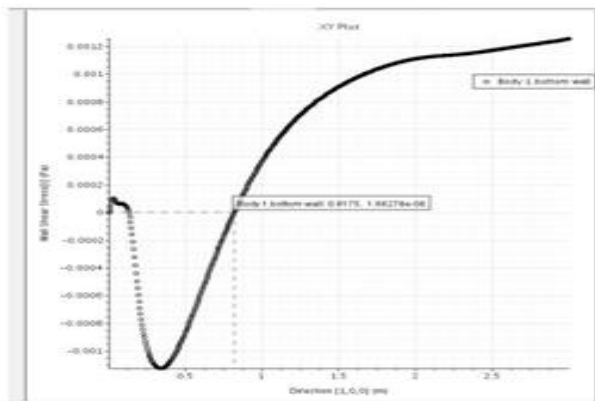


Figure 30: Reattachment length of K-omega model

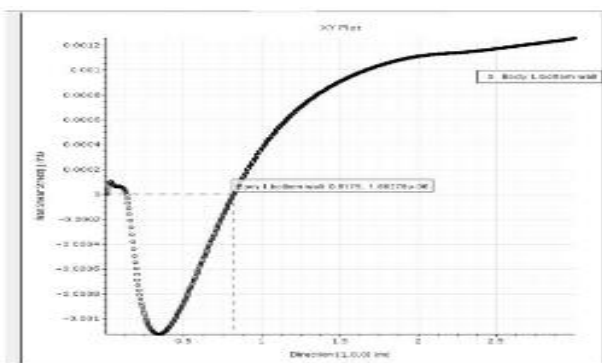


Figure 31: Reattachment length of K-epsilon model

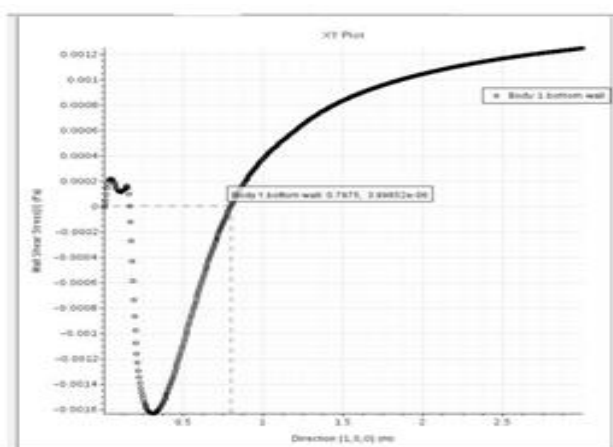


Figure 32: Reattachment length of Spalart –Allmaras Model